



ELSEVIER

Available online at www.sciencedirect.com

SCIENCE @ DIRECT®

Global and Planetary Change 49 (2005) 63–74

GLOBAL AND PLANETARY
CHANGE

www.elsevier.com/locate/gloplacha

Sensitivity of Cenozoic Antarctic ice sheet variations to geothermal heat flux

David Pollard^{a,*}, Robert M. DeConto^{b,1}, Andrew A. Nyblade^{c,2}

^a*Earth and Environmental Systems Institute, Pennsylvania State University, University Park, PA 16802, United States*

^b*Department of Geosciences, University of Massachusetts, Amherst, MA 01003, United States*

^c*Department of Geosciences, College of Earth and Mineral Sciences, Pennsylvania State University, University Park, PA 16802, United States*

Received 1 September 2004; accepted 24 May 2005

Abstract

The sensitivity of long-term Cenozoic variations of the East Antarctic ice sheet to geothermal heat flux is investigated, using a coupled climate–ice sheet model with various prescribed values and patterns of geothermal heat flux. The sudden growth of major ice across the Eocene–Oligocene boundary (~34 Ma) is used as a test bed for this sensitivity. A suite of several million year-long simulations spanning the transition is performed, with various geothermal heat flux magnitudes and spatial distributions reflecting current uncertainty. The climate–ice sheet model simulates the Eocene–Oligocene transition realistically as a non-linear ice-sheet response to orbital perturbations and a long-term gradual decline of atmospheric CO₂. It is found that reasonable variations of geothermal heat flux have very little effect on overall ice volumes and extents, and on the timing of major ice transitions. However, they cause large changes in basal areas at the pressure melting point at a given time, which could strongly influence other aspects of Cenozoic Antarctic evolution such as basal hydrology, sediment deformation and discharge, subglacial lakes, and basal erosional forms.

© 2005 Elsevier B.V. All rights reserved.

Keywords: Antarctica; Cenozoic; ice sheets; geothermal heat flow

1. Introduction

Physical properties at the base of the East and West Antarctic ice sheets (EAIS, WAIS) are largely unknown, probed only by radar and seismic means (e.g., Anandakrishnan et al., 1998; Bentley et al., 1998; Blankenship et al., 2001; Siegert, 1999, 2000a; Rippin et al., 2003) and by cores in West Antarctic ice streams (e.g., Engelhardt and Kamb,

* Corresponding author. Tel.: +1 814 865 2022; fax: +1 814 865 3191.

E-mail addresses: pollard@essc.psu.edu (D. Pollard), deconto@geo.umass.edu (R.M. DeConto), andy@geosc.psu.edu (A.A. Nyblade).

¹ Tel.: +1 413 545 3426.

² Tel.: +1 814 863 8341.

1997; Kamb, 2001). There is thus considerable uncertainty in prescribing basal quantities and verifying basal predictions of large-scale ice-sheet models of Antarctica (e.g., Warner and Budd, 1998; Fastook and Prentice, 1994; Huybrechts, 1990, 1993, 2002; Huybrechts et al., 2004; Ritz et al., 1997, 2001). Factors such as fine-scale basal roughness, distribution of deformable sediment versus hard bedrock, melting versus freezing and basal hydrology are all largely unknown. The main focus of modeled basal quantities to date has been the extent of thawed versus frozen beds (Huybrechts, 1990, 1993; Wilch and Hughes, 2000; Siegert, 2001; Pollard and DeConto, 2003; and other sensitivity studies noted below).

One uncertain basal input in these models is the geothermal heat flux. Its general magnitude for Antarctica is thought to be $\sim 50 \text{ mW m}^{-2}$, which is comparable to the vertical conductive heat flux through a thick polar ice sheet with a warm bed ($\sim 2 \text{ W m}^{-1} \text{ K}^{-1} \times 30 \text{ K} / 3000 \text{ m} = 20 \text{ mW m}^{-2}$). Thus the geothermal flux can potentially have a strong influence on basal temperatures, basal areas at the pressure melting point, and the production of liquid water (if not balanced by ice-sheet conductive or advective heat fluxes, the geothermal flux melts several mm of basal ice per year). The distribution of melting versus frozen beds and the amount of liquid water at the base are recognized as key factors in ice-sheet and glacial behavior, strongly affecting basal sliding and hydrology (e.g., Alley, 1989; Boulton et al., 1995), deformation and spatial distribution of soft basal sediment (Siegert, 2000a; Pollard and DeConto, 2003), erosion of hard bedrock and erosional forms (Rippin et al., 2003), and the distribution of subglacial lakes (Siegert and Dowdeswell, 1996; Siegert et al., 2001). They could affect large-scale ice-sheet evolution through periodic surging on $\sim 10^3$ to 10^5 year time scales (MacAyeal, 1992, 1993; Alley and MacAyeal, 1994; Clark et al., 1996; Licciardi et al., 1998; Marshall and Clarke, 2002). The geothermal heat flux can also influence ice-sheet configuration by changing internal ice temperatures and thus ice viscosity, but this would generally be more subtle and gradual compared to the effects of basal melting versus freezing.

This paper presents sensitivity experiments to test how much the current uncertainty in Antarctic geothermal heat flux affects the simulated long-term

Cenozoic evolution of the EAIS. We use a 3-D climate–ice sheet model previously applied to drastic variations in ice volume across the Eocene–Oligocene (E–O) boundary (DeConto and Pollard, 2003a,b). Three long-term simulations are compared, two using spatially uniform geothermal values bracketing the consensus range, and the third using a new distributed map based on geologic orogens as described below.

Several recent modeling studies have varied the geothermal flux systematically in 3-D ice-sheet simulations, and found it to be a useful diagnostic of model behavior. Ritz et al. (1997, 2001) used a range of spatially uniform values between 42 and 60 mW m^{-2} for future Greenland and Quaternary Antarctic ice sheets, and found little effects on overall ice volume and extent, and slight thinning of the central Antarctic plateau. Kerr and Huybrechts (1999) note a similar conclusion. Hansen and Greve (1996) used a larger range of uniform geothermal fluxes (42 to 105 mW m^{-2}) in their 3-D polythermal model of modern Antarctica, again finding no drastic changes in volume and geometry, but large variations in the extent of basal regions at the melt point. Takeda et al. (2002) used a spatially inhomogeneous geothermal flux, with a higher value under the WAIS (65 mW m^{-2}) than under the EAIS (54.6 mW m^{-2}) in recognition of the younger ages of West Antarctic rocks (Van der Wateren and Cloetingh, 1999). Again they found little change in ice volume and geometry, but significant increase in WAIS basal melt area compared to using a uniform 54.6 mW m^{-2} flux everywhere. All these simulations have been relatively short; the longer-term sensitivity over millions of years, with arguably more opportunity for non-linear response through a major transition such as the E–O boundary, has not been studied before to our knowledge.

There is considerable geophysical interest in the distribution of Antarctic geothermal heat flux per se (see Section 4). If differences in geothermal heat flux are found to strongly affect long-term ice-sheet evolution, then useful constraints can potentially be inferred from known Antarctic ice-sheet history. This would be complicated by other uncertainties in ice sheet processes such as basal hydrology and past surface budgets, but could still be feasible if the various effects on ice-sheet evolution can be distinguished.

2. Eocene–Oligocene transition

The Eocene–Oligocene transition provides a good testbed for the sensitivity of Antarctic ice-sheet evolution to geothermal heat flux, since the ice variations are large, and span the range from very little ice to full continental ice cover. Variations of global ice-sheet volume and ocean temperatures throughout the Cenozoic are deduced primarily from deep-sea core records of $\delta^{18}\text{O}$ and Mg/Ca in benthic foraminifera (Zachos et al., 2001; Lear et al., 2000, 2004). These data suggest several large fluctuations of the Antarctic ice sheet during the last few tens of millions of years, but the largest and most well known is the first widespread glaciation of Antarctica at the Eocene–Oligocene boundary. After millions of years with little or no ice, large ice sheets formed on Antarctica at ~34 Ma within a hundred thousand years (Zachos et al., 1996). This sudden growth has been hypothesized to be caused by the opening of Southern Ocean tectonic gateways, allowing the Antarctic Circum-Polar Current to thermally isolate Antarctica (Kennett, 1977; Exon et al., 2001). However, recent coupled-model simulations suggest that a more robust and likely cause is gradual cooling due to declining atmospheric CO_2 that triggered non-linear Height–Mass Balance Feedback (HMBF) of the ice sheet (DeConto and Pollard, 2003a,b), which produces a sudden jump in ice-sheet size as a geometrical consequence of the intersection of the ice-surface profile with the lowering climatic snowline (Oerlemans, 2002, Pollard and DeConto, 2005). Here we perform a sensitivity study using this coupled model, run for several million years across the Eocene–Oligocene transition and into its stable aftermath, to investigate the effects of different geothermal heat flux distributions on the predicted ice sheets.

3. Models and coupling methods

The models, boundary conditions, and coupling are described in more detail in DeConto and Pollard (2003a,b) and Pollard and DeConto (2003). Briefly, the GENESIS version 2 Global Climate Model (GCM) is run with T31 horizontal resolution (~3.75°) to simulate a suite of climates for the Cenozoic, with prescribed idealized orbital cycles and var-

ious CO_2 levels. The stored monthly climate fields are then downscaled to the fine-grid (40-km) topography of the Antarctic ice sheet, in order to calculate the annual surface mass balance that drives a 3-D dynamic ice-sheet model continuously through several million years.

3.1. Global climate model

The GENESIS global climate model consists of an atmospheric general circulation model (AGCM) with 18 vertical layers, coupled to multi-layer models of vegetation, soil or land ice, and snow, and a 50-m ocean slab with dynamic sea ice (Thompson and Pollard, 1997). The simulated present day climatology of version 2 is reasonably realistic for a medium-resolution GCM, (Thompson and Pollard, 1997; Mathieu et al., 2002), and its paleoclimate simulations have been validated against observations for a variety of periods (e.g., Pollard and Thompson, 1997; Pollard et al., 1998; Pinot et al., 1999; Doherty et al., 2000; Kageyama et al., 2001; Wang et al., 2004). The spatial distributions and overall surface ice-mass budgets over modern Greenland and Antarctica are well simulated for GCMs (Thompson and Pollard, 1997; Pollard and PMIP participating groups, 2000) and are reasonable over Northern Hemispheric ice sheets at Last Glacial Maximum (Pollard and Thompson, 1997). The Cenozoic GCM simulations in this paper use the reconstruction of Hay et al. (1999) of early Oligocene geography, topography and sea level.

3.2. Ice sheet model

A standard 3-D dynamic ice-sheet model is used over the Antarctic continent, following the established lineage of Huybrechts (1990, 1993, 1994), Ritz et al. (1997) and others. The ice model is run on a 40-km polar stereographic grid, with 10 vertical levels and a timestep of 10 to 20 years. Ice temperatures are predicted mainly for their effects on ice rheology and basal conditions. Vertical diffusive temperature profiles are also predicted through the upper ~2 km of bedrock, using 6 unequal levels and prescribed geothermal heat flux into the lowest bedrock layer. There are no ice shelves, and ice is removed seaward of the continental shoreline. The bedrock response to ice load is a local relaxation to isostatic

equilibrium with a time constant of 5000 years, and with the load modified by lithospheric flexure (Brotchie and Sylvester, 1969). Initial ice-free topography for the Cenozoic is prescribed from modern observed Antarctic bedrock elevations (Bamber and Bindschadler, 1997), isostatically rebounded with present ice removed.

The treatment of basal sliding is important since it is the primary means by which geothermal heat flux affects ice flow. As in other models, basal sliding can only occur where the bed is at the melt point and there is presumably enough liquid water to allow sliding. Here the sliding velocity is proportional to the square of the driving stress $\rho g H \nabla h$, where ρ is ice density, g is gravitational acceleration, H is ice thickness and ∇h is ice surface slope (e.g., Ritz et al., 1997). There is no other consideration of basal hydrology or deforming beds in these experiments (c.f., Pollard and DeConto, 2003). As discussed further below, basal sliding is important in our Cenozoic simulations, accounting for ~20 to 25% of the total ice mass flow averaged over the domain.

It should be noted that the ice model is limited to the terrestrial East Antarctic Ice Sheet (EAIS). Formation of the marine-based West Antarctic Ice Sheet (WAIS) is prevented in the model by the absence of ice shelves or calving fronts. This probably has only small effects on our Cenozoic EAIS simulations, due to the Transantarctic Mountains forming a partial barrier between the two; moreover, the WAIS may not have existed at all until later in the Cenozoic (Scherer, 1991).

3.3. GCM–ice sheet coupling

GCM monthly mean air temperatures and precipitation are bilinearly interpolated to the finer ice-sheet grid, and vertically corrected to the ice surface elevations using constant lapse rate assumptions (Thompson and Pollard, 1997). A positive-degree day parameterization is used to calculate the net annual surface mass balance with allowance for diurnal cycles, superimposed ice and refreezing of meltwater (e.g., Ritz et al., 1997; Marshall and Clarke, 1999). This calculation is repeated every 200 years as the ice surface varies.

Since it is computationally infeasible to run the GCM continuously over geologic time scales, the coupling between the climate and ice-sheet models

is necessarily asynchronous. The procedure used here is explained in more detail in DeConto and Pollard (2003a,b). In the first preliminary step, relatively short 40 kyr simulations are performed with varying orbital parameters and fixed atmospheric CO₂. A synthetic orbital sequence is used with precession, obliquity and eccentricity varying sinusoidally with periods of 20, 40 and 80 kyr, respectively (DeConto and Pollard, 2003b, their Fig. 3). This captures the essence of orbital forcing (the dominant ~100 kyr periodicity of real eccentricity is shifted to 80 kyr to achieve a repeating pattern). As in traditional asynchronous coupling, the ice-sheet model is integrated continuously through each 40 kyr simulation, starting with no ice. The GCM is run for a few decades at the start of each run, and again every 10 kyr with updated ice-sheet size and orbit parameters to provide mass balance for the ice model. Monthly mean temperatures and precipitation from the five GCM snapshots are stored for later use. Two such GCM suites are generated with different atmospheric CO₂ levels, 2× and 3× PAL (pre-industrial atmospheric level, taken as 280 ppmv).

Subsequently, the stored suites of monthly meteorologic GCM variables are weighted appropriately to provide the climate and surface mass balance at any time as the ice-sheet model is integrated continuously through millions of years. The same synthetic 40-kyr orbital sequence is repeated in alternating forward and backward passes, to produce a smooth 80-kyr eccentricity cycle. The ice-driving GCM climatology (temperature, precipitation) is linearly weighted in time between the appropriate stored orbital solutions of the preliminary simulations described above. To account for the imposed long-term trend in CO₂, interpolation/extrapolation is also performed between the two GCM suites for 2× and 3× PAL, with respect to log(CO₂) to account for its logarithmic radiative effect. Although this procedure roughly captures some albedo feedback due to higher-frequency ice-sheet and sea-ice variability in response to orbital cycles, in general it does not account for terrestrial ice-albedo feedback in the long-term simulations. This is especially true across major ice transitions such as the Eocene–Oligocene boundary, where the ice-sheet expansion in the long-term simulation does not correspond at all to the ice sheets in the GCM sequences. However, since varying ice-sheet topography is

accounted for in the surface mass balance computations every 200 years, height–mass balance feedback is captured adequately.

4. Geothermal heat flux

In our sensitivity experiments, we investigate three spatial distributions of geothermal heat flux derived from geologic models for East Antarctica. Most models assume that East Antarctica has existed as a coherent continental block (shield) with an Archean nucleus since before the assembly of the Rodinia supercontinent (~1000 Ma) (Tingey, 1991; Dalziel, 1991; Rogers et al., 1995). This view is based on the widespread occurrence of Archean and Proterozoic outcrops along the East Antarctic coast (Tingey, 1991) and the presence of similar Proterozoic rocks in the Transantarctic mountains (Goodge et al., 2001). Other studies suggest a more complicated tectonic history for East Antarctica, including multiple Proterozoic/early Paleozoic orogenic events. Cambrian rocks outcrop near the Lambert Graben in the Southern Prince Charles Mountains (Boger et al., 2001), and Fitzsimons (2000, 2004) suggests that these outcrops are related to the 550–500 Ma Australian Pinjarra Orogen and may form a suture zone extending into the interior of East Antarctica beneath the Gamburtsev Subglacial Mountains. This suggestion is consistent with the results of the studies by Studinger et al. (2003a,b) showing evidence for an ancient (Proterozoic) suture zone in the Lake Vostok region.

The first heat flux distribution we use, a uniform 37.7 mW m^{-2} over Antarctica, is the same as used by DeConto and Pollard (2003a). This distribution represents an end member case where the entire East Antarctic craton is comprised of Archean lithosphere and the effect of possibly higher geothermal heat flux from West Antarctica is assumed to be negligible because of the much smaller area. The global average heat flow for Archean cratons is 41 ± 11 (s.d.) mW m^{-2} (Nyblade, 1999), and therefore the heat flow of 37.7 mW m^{-2} used in our model is within the lower range of heat flow expected from an Archean craton.

The second heat flux distribution we use is a uniform 75.4 mW m^{-2} , double the heat flux in the first model. This distribution represents the other end member case where the entire East Antarctic craton is

comprised of Proterozoic lithosphere with high heat production in the crust. Heat flow from Proterozoic lithosphere is typically higher than from Archean lithosphere, but is variable depending on crustal heat production and proximity to the margins of Archean lithosphere (Pollack et al., 1993; Nyblade, 1999; Artemieva and Mooney, 2001), ranging from as low as $\sim 40 \text{ mW m}^{-2}$ in some Paleoproterozoic mobile belts adjacent to Archean cratons to as high as $70\text{--}75 \text{ mW m}^{-2}$ in Neoproterozoic mobile belts with high crustal heat production far away from an Archean craton (Nyblade and Pollack, 1993; Nyblade, 1999).

The third heat flux distribution we use varies spatially and represents a more realistic distribution compared to the two end member cases. In this distribution (Fig. 1), we extend the Archean Mawson craton into the interior of East Antarctica, following the reconstruction of Fitzsimons (2004) and assign to it a heat flow of 41 mW m^{-2} , typical for Archean lithosphere (Nyblade, 1999). The rest of East Antarctica we assume to be Proterozoic, again following the reconstruction of Fitzsimons (2004), and assign to it a heat flow of 55 mW m^{-2} , a mid-range value for Proterozoic lithosphere (Nyblade, 1999). We assign a slightly higher heat flow of 60 mW m^{-2} to the

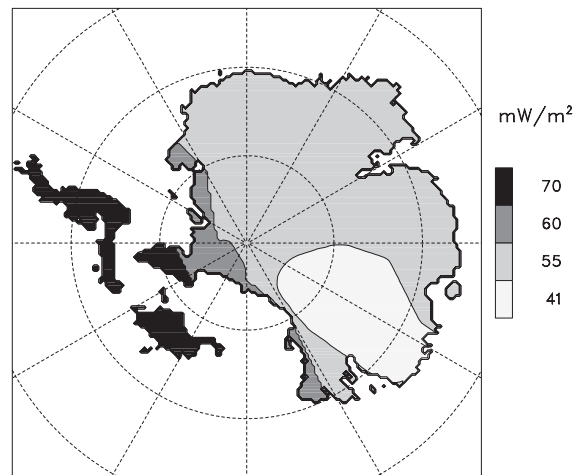


Fig. 1. Prescribed geothermal heat flux (mW m^{-2}) used in the third ice-sheet model sensitivity experiment. The pattern is based on orogen distributions, with West Antarctic=70, Transantarctic=60, Mawson Craton and similar ages=41, and East African, Pinjarra, Albany–Fraser–Wilkes and Ross–Delamerian=55. Latitude circles are shown at 80°S , 70°S and 60°S , and the 0° longitude line runs vertically upwards (also in Figs. 3 and 4).

Transantarctic Mountains, reflecting the Neoproterozoic age of the basement provinces found there, and a heat flow of 70 mW m^{-2} to West Antarctica, reflecting the possible Mesozoic–Cenozoic origin of the West Antarctic rift system (Lawver et al., 1991; Fitzgerald and Baldwin, 1997).

Siegert (2000b) used a simple thermal model to estimate geothermal heat flux at many observed subglacial lakes under Antarctic ice, and found values varying between 37 and 65 mW m^{-2} , quite comparable to the range in Fig. 1. There is some broad agreement between the two distributions (such as higher values in and near the Transantarctics), but regional details differ, as expected given the considerable uncertainties in both methods.

As mentioned above, geothermal heat flux is applied at the base of the ice-sheet model's 2-km thick bedrock component, and its effect is quickly transmitted ($\sim 10^5$ years) upwards to the ice, where it influences ice-sheet dynamics through its effect on basal and internal ice temperatures. The basal effect in our model is generally more pronounced, allowing basal sliding between the ice and the bed where the basal temperature reaches the pressure melting point.

5. Ice sheet results

Fig. 2 shows the variation of total ice volume through the 6-million year duration of the runs. As in

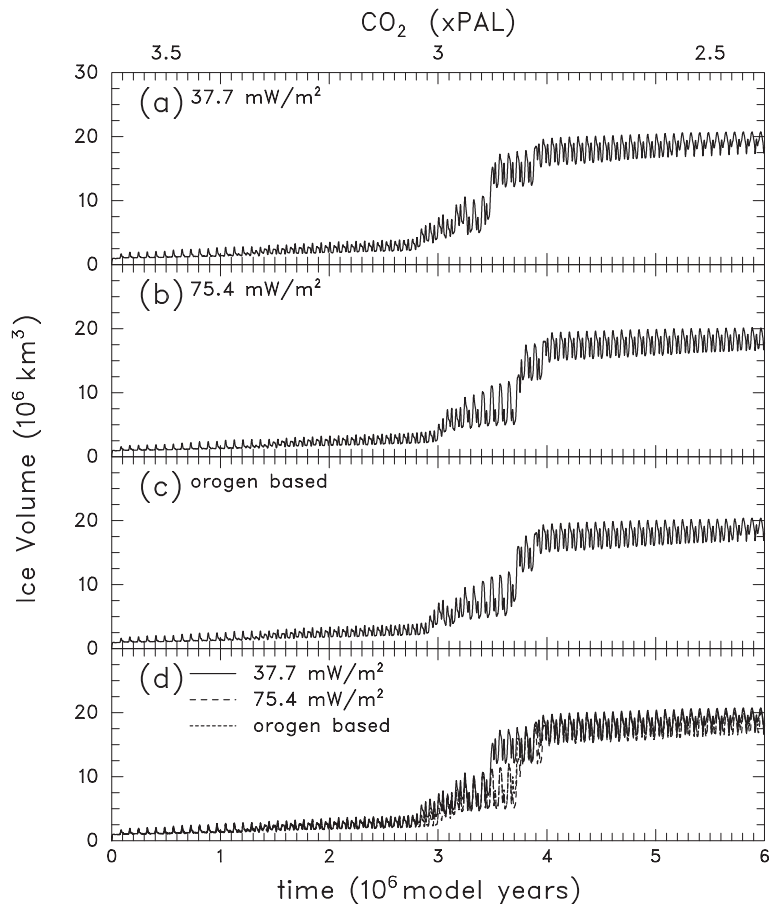


Fig. 2. Total Antarctic ice volumes in long-term simulations across the Eocene–Oligocene boundary, starting from an ice-free state, with three different geothermal heat flux distributions: (a) Uniform, 37.7 mW/m^2 . (b) Uniform, 75.4 mW/m^2 . (c) Spatially varying based on orogen distributions. (d) All three simulations superimposed. The top axis indicates the prescribed linear decline in atmospheric CO_2 , relative to the Preindustrial Atmospheric Level of 280 ppmv.

DeConto and Pollard (2003a), a gradual linear decline of atmospheric CO_2 is prescribed, more or less consistent with estimates from geochemical models (Bernier and Kothavala, 2001) and deep-sea core data (Pagani et al., 1999; Pearson and Palmer, 2000; Retallack, 2001, 2002; but see Royer et al., 2001; Demicco et al., 2003). The gradual cooling results in relatively sudden and drastic ice-sheet growth when CO_2 levels fall slightly below $3\times$ pre-industrial levels ($\sim 3\times 280$ ppmv). The high frequency oscillations are due to orbital forcing.

The three different geothermal heat flux regimes have very little effect on total ice amounts, and the amplitude and timing of the main transition are essentially unchanged. There are slight differences in the timings of individual ice-cap growth (bottom panel), but these reflect more the extremely non-linear nature of height–mass balance feedback that produces essentially stochastic behavior during the transition.

Figs. 3 and 4 show ice sheet surface elevations and areas of basal melt at two particular times during the

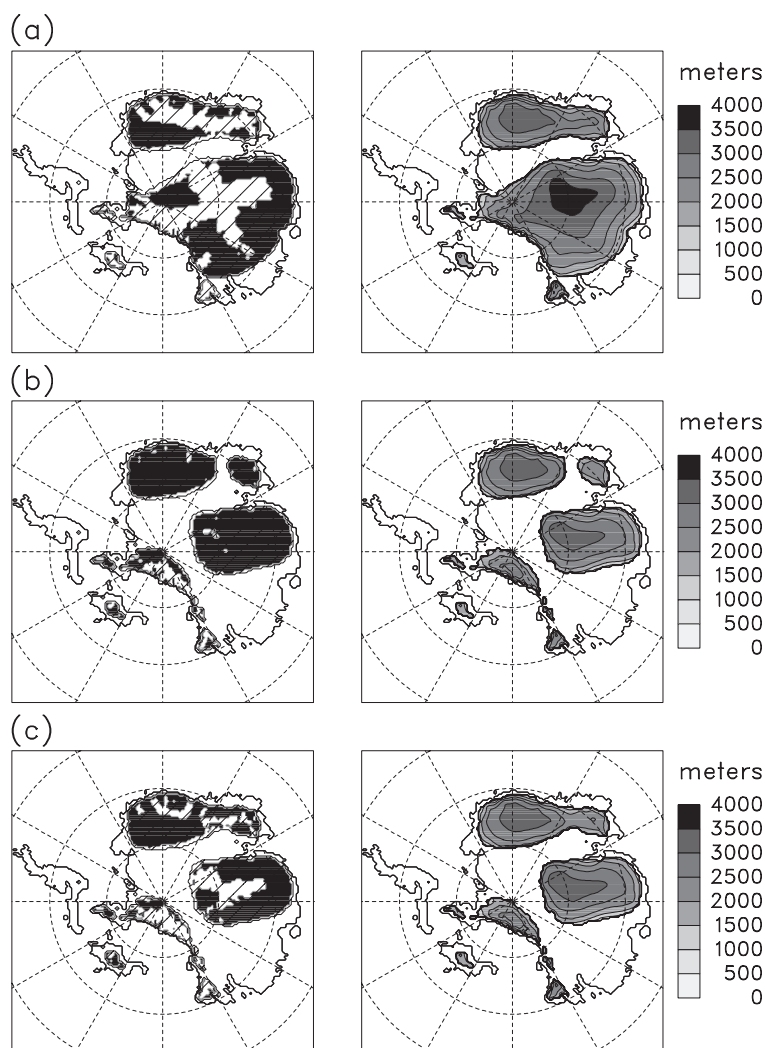


Fig. 3. Areas of the ice-sheet base at the pressure-melting point (left-hand column, dark areas) and ice-sheet surface elevation (right-hand column, meters), at 3.6 million years after the start of the simulations shown in Fig. 2. Shading in the left-hand panels shows the current ice sheet extent. The three rows correspond to our three geothermal heat flux distributions: (a) Uniform, 37.7 mW/m^2 . (b) Uniform, 75.4 mW/m^2 . (c) Spatially varying based on orogen distributions.

runs. As might be expected from above, the spatial distributions of ice are influenced very little by the geothermal heat flux. This is despite the substantial contribution of basal sliding to the overall ice-sheet flow (~20 to 25% overall for the larger ice sheets after the first 3 million years), extensive bed areas at the melt point, and significant differences in these melt areas between experiments (Figs. 3 and 4, left-hand columns). During the transition (Fig. 3) the differences reflect more the stochastic nature of the fluctuations, and particular snapshots at closely spaced times (not shown) do not show any systematic effect of

geothermal heat flux. In the stable period following the transition (Fig. 4), with a single continental ice sheet, there is a discernible effect of slightly thicker ice over the Queen Maud mountains (Atlantic sector) and Gamburtsev mountains (central plateau) caused by lower geothermal heat flux (Fig. 4). However, the differences in marginal extent and total volume are still very small.

Figs. 3 and 4 also show the extents of basal regions at the melt point (cf., Huybrechts, 1990, his Fig. 8; Hansen and Greve, 1996, their Fig. 3). Here, there are substantial differences between the

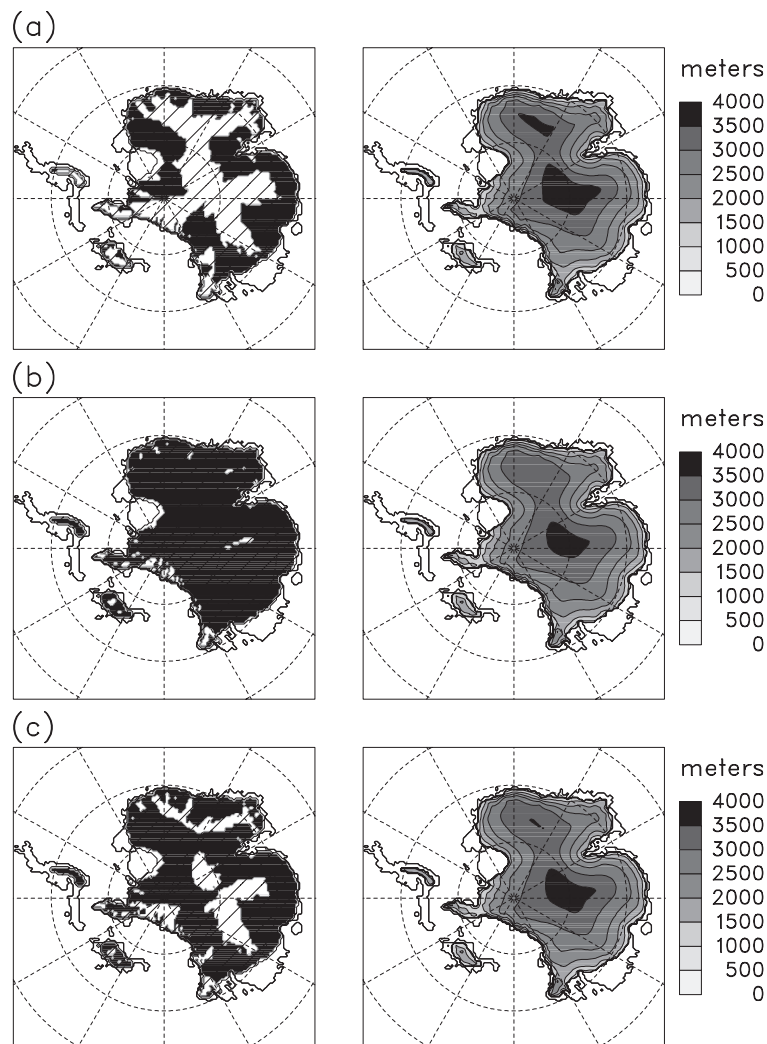


Fig. 4. As Fig. 3 except at 6 million years after the start of the simulations.

geothermal heat flux cases. With the lowest uniform value (Figs. 3a and 4a), the interior regions are nearly all frozen to the bed, compared to nearly all at the melt point with the doubled uniform value (Figs. 3b and 4b). The greatest differences are seen where the ice is thickest, as expected since surface temperatures (nearly the same between the cases) there have less influence on the base. With spatially varying geothermal heat flux (Figs. 3c and 4c), basal conditions are intermediate between the two uniform cases; the boundaries between melting and freezing seem to be mainly determined by ice and bedrock configuration, since there is not any obvious correspondence with the heat-flux/orogen patterns shown in Fig. 1. Nevertheless, these results demonstrate the importance of reasonably accurate knowledge of geothermal heat flux for the prediction of basal melting.

6. Conclusions

Within the consensus range of uncertainty in geothermal heat flux under the Antarctic, the effects on long-term evolution of the East Antarctic Ice sheet are very small, in terms of overall ice volume and extent. This is true both for the uncertainty in the overall continent-wide value (~ 40 to 80 mW m^{-2}), and for spatial variations such as in Fig. 1. It holds both for relatively quiescent periods in the Cenozoic, and across more abrupt transitions such as the Eocene–Oligocene boundary, where the ice sheet responds sensitively and non-linearly to external forcing.

However, differences in geothermal heat flux cause large differences in the basal areas at the pressure-melting point at a given time, as found previously by Hansen and Greve (1996). As noted above, differences in basal melting extents as large as those in Figs. 3 and 4 are likely to be important for many studies concerned with Antarctic basal processes, such as ice streams and basal hydrology (Budd and Jenness, 1987; Vogel et al., 2003), erosional forms (Rippin et al., 2003), sub-glacial lake history (Siegert et al., 2001), evolution of deforming sediment (Siegert, 2000a; Pollard and DeConto, 2003), and possible regional surging (MacAyeal, 1992).

These conclusions are much the same as those found in earlier ice-sheet/heat-flux studies mentioned

in the Introduction. Our simulations are much longer in duration, and pass through a major non-linear transition from small to large ice sheets. Therefore, contrary to our results, one might have expected greater sensitivity of ice-sheet evolution to geothermal heat flux. That this is not the case seems to be due to the dominant control of Height–Mass Balance Feedback during the major transition. For a given CO_2 level, there is a critical ice size beyond which individual Antarctic ice caps expand non-linearly into a continental ice sheet (DeConto and Pollard, 2003a; Pollard and DeConto, 2005). For instance, even if larger geothermal heat flux produces noticeably smaller ice caps before the transition, this only delays the onset of the transition by a few orbital cycles until the gradually declining CO_2 level compensates for the lower ice surface elevations (as seen in Fig. 2d for low versus high geothermal flux around 3.6 to 3.8 million years).

Here and in many previous models, geothermal heat flux affects basal sliding via the simple all-or-nothing switch of whether the basal temperature is at or below the pressure-melting point. Thus the sensitivity is limited to the lateral extent that the basal melt-point isotherm is shifted by different geothermal heat fluxes. If this isotherm moves only slightly, then more complex basal sliding physics could potentially provide greater sensitivity, such as a dependence on the amount of basal water. However, as discussed above, this isotherm (or equivalently the basal area at the melt point) is strongly affected by geothermal heat flux variations, suggesting that the simplicity of the sliding parameterization is not overly restricting the sensitivity of ice volume to geothermal heat flux. Nevertheless, this topic should be addressed in future work using models with explicit basal hydrology.

Our conclusions apply to the terrestrial East Antarctic Ice Sheet (EAIS). As noted above, a marine-based West Antarctic Ice Sheet (WAIS) cannot form in the model used here due to the absence of ice shelves and calving fronts. This may be reasonable for the E–O boundary if the WAIS had not formed by that time (Scherer, 1991). Later in the Cenozoic, WAIS variability especially in the vicinity of the West Antarctic ice streams and grounding lines might be sensitive to the local geothermal heat flux (cf., Takeda et al., 2002).

Acknowledgments

We are grateful to Catherine Ritz and an anonymous reviewer for constructive reviews and suggestions. This research was funded in part by the US National Science Foundation under collaborative grant No. ATM-9905890/9906663.

References

- Alley, R.B., 1989. Water-pressure coupling of sliding and bed deformation: I. Water System. *J. Glaciol.* 35, 108–118.
- Alley, R.B., MacAyeal, D.R., 1994. Ice-rafted debris associated with binge-purge oscillations of the Laurentide Ice Sheet. *Paleoceanography* 9, 503–511.
- Anandkrishnan, S., Blankenship, D.D., Alley, R.B., Stoffa, P.L., 1998. Influence of subglacial geology on the position of a West Antarctic ice stream from seismic measurements. *Nature* 394, 62–65.
- Artemieva, I.M., Mooney, W.D., 2001. Thermal thickness and evolution of Precambrian lithosphere: a global study. *J. Geophys. Res.* 106, 16387–16414.
- Bamber, J.A., Bindshadler, R.A., 1997. An improved elevation dataset for climate and ice-sheet modeling: validation with satellite imagery. *Ann. Glaciol.* 25, 439–444.
- Bentley, C.R., Lord, N., Liu, C., 1998. Radar reflections reveal a wet bed beneath stagnant ice stream C and a frozen bed beneath ridge BC, West Antarctica. *J. Glaciol.* 44, 149–156.
- Berner, R.A., Kothavala, Z., 2001. GEOCARB III: a revised model of atmospheric CO₂ over Phanerozoic time. *Am. J. Sci.* 301, 182–204.
- Blankenship, D.D., Morse, D.L., Finn, C.A., Bell, R.E., Peters, M.E., Kempf, S.D., Hodge, S.M., Studinger, M., Behrendt, J.C., Brozena, J.M., 2001. Geologic controls of the initiation of rapid basal motion for West Antarctic ice streams: a geophysical perspective including new airborne radar sounding and laser altimetry results. In: Alley, R.B., Bindshadler, R.A. (Eds.), *The West Antarctic Ice Sheet: Behavior and Environment*, Antarctic Research Series, vol. 77. American Geophysical Union, Washington D.C., pp. 105–121.
- Boger, S.D., Wilson, C.J.L., Fanning, C.M., 2001. Early Paleozoic tectonism within the East Antarctic craton: the final suture between east and west Gondwana? *Geology* 29, 463–466.
- Boulton, G.S., Caban, P.E., van Gijssel, K., 1995. Groundwater flow beneath ice sheets. Part I — large scale patterns. *Quat. Sci. Rev.* 14, 545–562.
- Brotchie, J.F., Sylvester, R., 1969. On crustal flexure. *J. Geophys. Res.* 74, 5240–5252.
- Budd, W.F., Jennesen, D., 1987. Numerical modeling of the large-scale basal water flux under the West Antarctic Ice Sheet. In: van der Veen, C.J., Oerlemans, J. (Eds.), *Dynamics of the West Antarctic Ice Sheet*. D. Reidel, Dordrecht, pp. 293–320.
- Clark, P.U., Alley, R.B., Keigwin, L.D., Licciardi, J.M., Johnsen, S.J., Wang, H., 1996. Origin of the first global meltwater pulse following the last glacial maximum. *Paleoceanography* 11, 563–577.
- Dalziel, I.W.D., 1991. Pacific margins of Laurentia and East Antarctica–Australia as a conjugate rift pair: evidence and implications for an Eocambrian supercontinent. *Geology* 19, 598–601.
- DeConto, R.D., Pollard, D., 2003a. Rapid Cenozoic glaciation of Antarctica triggered by declining atmospheric CO₂. *Nature* 421, 245–249.
- DeConto, R.D., Pollard, D., 2003b. A coupled climate–ice sheet modeling approach to the early Cenozoic history of the Antarctic ice sheet. *Palaeogeogr. Palaeoclim. Palaeoecol.* 198, 39–52.
- Demicco, R., Lowenstein, T.K., Hardie, L.A., 2003. Atmospheric pCO₂ since 60 Ma from records of seawater pH, calcium and primary carbonate mineralogy. *Geology* 31, 793–796.
- Doherty, R., Kutzbach, J., Foley, J., Pollard, D., 2000. Fully coupled climate/dynamical vegetation model simulations over Northern Africa during the mid-Holocene. *Clim. Dyn.* 16, 561–573.
- Engelhardt, H., Kamb, B., 1997. Basal hydraulic system of a West Antarctic ice stream: constraints from borehole observations. *J. Glaciol.* 43, 207–230.
- Exon, N.F., Kennett, J.P., Malone, M.J., et al., 2001. Proceedings of the Ocean Drilling Program, Initial Reports, vol. 189. (http://www-odp.tamu.edu/publications/189_IR/189ir.htm).
- Fastook, J.L., Prentice, M., 1994. A finite-element model of Antarctica: sensitivity test for meteorological mass–balance relationship. *J. Glaciol.* 40, 167–175.
- Fitzgerald, P., Baldwin, S., 1997. Detachment fault model for the evolution of the Ross Embayment. In: Ricci, C.A. (Ed.), *The Antarctic Region: Geological Evolution and Processes*, pp. 555–564.
- Fitzsimons, I.C.W., 2000. Grenville-age basement provinces in East Antarctica: evidence for three separate collisional orogens. *Geology* 28, 879–882.
- Fitzsimons, I.C.W., 2004. Proterozoic basement provinces of southern and southwestern Australia, and their correlation with Antarctica. In: Yoshida, M., Windley, B.F., Dasgupta, S. (Eds.), *Proterozoic East Gondwana: Supercontinent Assembly and Breakup*. Geological Society Spec. Publ., London.
- Godge, J.W., Fanning, C.M., Bennett, V.C., 2001. U–Pb evidence of 1.7 Ga crustal tectonism during the nimrod orogeny in the trans-Antarctic mountains, Antarctica: implications for Proterozoic plate reconstructions. *Precambrian Res.* 112, 261–288.
- Hansen, J., Greve, R., 1996. Polythermal modelling of steady states of the Antarctic ice sheet in comparison with the real world. *Ann. Glaciol.* 23, 382–387.
- Hay, W.W., DeConto, R.M., Wold, C.N., Wilson, K.M., Voight, S., Schulz, M., Wold-Rosby, A., Dullo, W.-C., Ronov, A.B., Balukhovskiy, A.N., 1999. An alternative global Cretaceous paleogeography. In: Barrera, E., Johnson, C. (Eds.), *The Evolution of Cretaceous Ocean Climate Systems*. Geol. Soc. Amer., Boulder, Colorado, pp. 1–48.
- Huybrechts, P., 1990. A 3-D model for the Antarctic ice sheet: a sensitivity study on the glacial–interglacial contrast. *Clim. Dyn.* 5, 79–92.
- Huybrechts, P., 1993. Glaciological modeling of the late Cenozoic East Antarctic icesheet: stability or dynamism? *Geog. Ann.* 75A, 221–238.

- Huybrechts, P., 1994. Formation and disintegration of the Antarctic ice sheet. *Ann. Glaciol.* 20, 336–340.
- Huybrechts, P., 2002. Sea-level changes at the LGM from ice-dynamic reconstructions of the Greenland and Antarctic ice sheets during the glacial cycles. *Quat. Sci. Rev.* 21, 203–231.
- Huybrechts, P., Gregory, J., Janssens, I., Wild, M., 2004. Modelling Antarctic and Greenland volume changes during the 20th and 21st centuries forced by GCM time slice integrations. *Glob. Planet. Change* 42, 83–105.
- Kageyama, M., Peyron, O., Tarasov, P., Pinot, S., Guiot, G., Ramstein, G., Joussaume, S., PMIP participating groups, 2001. The Last Glacial Maximum climate over Europe and Western Siberia: a PMIP comparison between models and data. *Clim. Dyn.* 17, 23–43.
- Kamb, W.B., 2001. Basal zone of the West Antarctic ice streams and its role in lubrication of their rapid motion. In: Alley, R., Bindschadler, R. (Eds.), *The West Antarctic Ice Sheet: Behavior and Environment*, Antarctic Research Series, vol. 77. American Geophysical Union, Washington D.C., pp. 157–199.
- Kerr, A., Huybrechts, P., 1999. The response of the East Antarctic ice sheet to the evolving tectonic configuration of the Transantarctic mountains. *Glob. Planet. Change* 23, 213–229.
- Kennett, J.P., 1977. Cenozoic evolution of Antarctic glaciation, the circum-Antarctic oceans and their impact on global paleoceanography. *J. Geophys. Res.* 82, 3843–3859.
- Lawver, L.A., Royer, J.Y., Sandwell, D.T., Scotese, C.R., 1991. Evolution of the Antarctic continental margin. In: Thomson, M., Crame, J., Thomson, J. (Eds.), *Geological Evolution of Antarctica*. Cambridge Univ. Press, New York, pp. 533–539.
- Lear, C.H., Elderfield, H., Wilson, P.A., 2000. Cenozoic deep-sea temperatures and global ice volumes from Mg/Ca in benthic foraminiferal calcite. *Science* 287, 269–272.
- Lear, C.H., Rosenthal, Y., Coxall, H.K., Wilson, P.A., 2004. Late Eocene to early Miocene ice sheet dynamics and the global carbon cycle. *Paleoceanography* 19, PA4015. doi: 10.1029/2004PA001039.
- Licciardi, J.M., Clark, P.U., Jenson, J.W., MacAyeal, D.R., 1998. Deglaciation of a soft-bedded Laurentide ice sheet. *Quat. Sci. Rev.* 17, 427–448.
- MacAyeal, D.R., 1992. Irregular oscillations of the West Antarctic ice sheet. *Nature* 359, 29–32.
- MacAyeal, D.R., 1993. Binge–purge oscillations of the Laurentide ice sheet as a cause of the North Atlantic's Heinrich Events. *Paleoceanography* 8, 775–784.
- Marshall, S.J., Clarke, G.K.C., 1999. Ice sheet inception: subgrid hypsometric parameterization of mass balance in an ice sheet model. *Clim. Dyn.* 15, 533–550.
- Marshall, S.J., Clarke, G.K.C., 2002. Basal temperature evolution of North American ice sheets and implications for the 100-kyr cycle. *Geophys. Res. Lett.* 29 (2214), 67-1–67-4. doi: 10.1029/2002GL015192.
- Mathieu, R., Pollard, D., Cole, J.E., White, J.W.C., Webb, R.S., Thompson, S.L., 2002. Simulation of stable water isotope variations by the GENESIS GCM for modern conditions. *J. Geophys. Res.*, [Atmos.] 107, D4. doi: 10.1029/2001JD900255.
- Nyblade, A.A., 1999. Heat flow and the structure of Precambrian lithosphere. *Lithos*, 81–91.
- Nyblade, A.A., Pollack, H.N., 1993. A global analysis of heat flow from Precambrian terrains: implications for the thermal structure of Archean and Proterozoic lithosphere. *J. Geophys. Res.* 98, 12207–12218.
- Oerlemans, J., 2002. On glacial inception and orography. *Quat. Int.* 95–96, 5–10.
- Pagani, M., Arthur, M.A., Freeman, K.H., 1999. Miocene evolution of atmospheric carbon dioxide. *Paleoceanography* 14, 273–292.
- Pearson, P.N., Palmer, M.R., 2000. Atmospheric carbon dioxide over the past 60 million years. *Nature* 406, 695–699.
- Pinot, S., Ramstein, G., Harrison, S.P., Prentice, I.C., Guiot, J., Stute, M., Joussaume, S., 1999. Tropical climates at the Last Glacial Maximum: comparison of Paleoclimate Modeling Inter-comparison Project (PMIP) simulations and paleodata. *Clim. Dyn.* 15, 857–874.
- Pollack, H.N., Hurter, S.J., Johnson, J.R., 1993. Heat flow from the Earth's interior: analysis of the global data set. *Rev. Geophys.* 31, 267–280.
- Pollard, D., DeConto, R.M., 2003. Antarctic climate and sediment flux in the Oligocene simulated by a climate–ice sheet–sediment model. *Palaeogeogr. Palaeoclimatol.* 198, 53–67.
- Pollard, D., DeConto, R.M., 2005. Hysteresis in Cenozoic Antarctic ice sheet variations. *Glob. Planet. Change* 45, 9–21.
- Pollard, D., PMIP participating groups, 2000. Comparisons of ice-sheet surface mass budgets from Paleoclimate Modeling Inter-comparison Project (PMIP) simulations. *Glob. Planet. Change* 24, 79–106.
- Pollard, D., Thompson, S.L., 1997. Climate and ice-sheet mass balance at the last glacial maximum from the GENESIS version 2 global climate model. *Quat. Sci. Rev.* 16, 841–863.
- Pollard, D., Bergengren, J.C., Stillwell-Soller, L.M., Felzer, B., Thompson, S.L., 1998. Climate simulations for 10000 and 6000 years BP using the GENESIS global climate model. *Palaeoclimates: Data and Modelling* 2, 183–218.
- Retallack, G.J., 2001. A 300-million-year record of atmospheric carbon dioxide from fossil plant cuticles. *Nature* 411, 287–290.
- Retallack, G.J., 2002. Carbon dioxide and climate over the past 300 Myr. *Philos. Trans. R. Soc. Lond.*, A 360, 659–673.
- Rippin, D.M., Bamber, J.L., Siegert, M.J., Vaughan, D.G., Corr, H.F.J., 2003. Basal topography and ice flow in the Bailey/Slessor region of East Antarctica. *J. Geophys. Res.* 108 (F1), 6008. doi: 10.1029/2003JF000039.
- Ritz, C., Fabre, A., Letreguilly, A., 1997. Sensitivity of a Greenland ice sheet model to ice flow and ablation parameters: consequences for the evolution through the last climate cycle. *Clim. Dyn.* 13, 11–24.
- Ritz, C., Rommelaere, V., Dumas, C., 2001. Modeling the evolution of Antarctic ice sheet over the last 420,000 years: implications for altitude changes in the Vostok region. *J. Geophys. Res.* 106 (D23), 31943–31964.
- Rogers, J.J., Unrug, R., Sultan, M., 1995. Tectonic assembly of Gondwana. *J. Geodyn.* 19, 1–34.
- Royer, D.L., Wing, S.L., Beerling, D.J., Jolley, D.W., Koch, P.L., Hickey, L.J., Berner, R.A., 2001. Paleobotanical evidence for near present-day levels of atmospheric CO₂ during part of the Tertiary. *Science* 292, 2310–2313.

- Scherer, R.P., 1991. Quaternary and Tertiary microfossils from beneath Ice Stream B — evidence for a dynamic West Antarctic ice sheet history. *Glob. Planet. Change* 90, 395–412.
- Siegert, M.J., 1999. On the origin, nature and uses of Antarctic ice-sheet radio-echo layering. *Prog. Phys. Geog.* 23, 159–179.
- Siegert, M.J., 2000a. Radar evidence of water-saturated sediments beneath the central Antarctic ice sheet. In: Maltman, A., Hambrey, M., Hubbard, B. (Eds.), *The Deformation of Glacial Materials*, *Geol. Soc. Special Publ.*, vol. 176, pp. 217–229.
- Siegert, M.J., 2000b. Antarctic subglacial lakes. *Earth-Sci. Rev.* 50, 29–50.
- Siegert, M.J., 2001. Comments on “Calculating the basal thermal zones beneath the Antarctic ice sheet”. In: Wilch, E., Hughes, T. (Eds.), *J. Glaciol.*, vol. 47, pp. 159–160.
- Siegert, M.J., Dowdeswell, J.A., 1996. Spatial variations in heat at the base of the Antarctic ice sheet from analysis of the thermal regime above subglacial lakes. *J. Glaciol.* 42, 501–509.
- Siegert, M.J., Ellis-Evans, J.C., Tranter, M., Mayer, C., Petit, J.-R., Salamatin, A., Priscu, J.C., 2001. Physical, chemical and biological processes in Lake Vostok and other Antarctic subglacial lakes. *Nature* 414, 603–609.
- Studinger, M., et al., 2003a. Ice cover, landscape setting, and geological framework of Lake Vostok, East Antarctica. *Earth Planet. Sci. Lett.* 205, 195–210.
- Studinger, M., Kamber, G.D., Bell, R.E., Levin, V., Raymond, C.A., Tikku, A.A., 2003b. Geophysical models for the tectonic framework of the Lake Vostok region, East Antarctica. *Earth Planet. Sci. Lett.* 216, 663–677.
- Takeda, A., Cox, S., Payne, A.J., 2002. Parallel numerical modeling of the Antarctic ice sheet. *Comput. Geosci.* 28, 723–734.
- Thompson, S.L., Pollard, D., 1997. Greenland and Antarctic mass balances for present and doubled CO₂ from the GENESIS v2 global climate model. *J. Clim.* 10, 871–900.
- Tingey, R.J., 1991. The regional geology of Archean and Proterozoic rocks in Antarctica. In: Tingey, R.J. (Ed.), *The Geology of Antarctica*. Clarendon Press, Oxford, UK, pp. 1–58.
- Van der Wateren, F.M., Cloetingh, S.A.P.L., 1999. Feedbacks of lithosphere dynamics and environmental change of the Cenozoic West Antarctic Rift System. *Glob. Planet. Change* 23, 1–24.
- Vogel, S.W., Tulaczyk, S., Joughin, I., 2003. Distribution of basal melting and freezing between tributaries of Ice Stream C, West Antarctica. *Ann. Glaciol.* 36, 273–282.
- Wang, G., Eltahir, E.A.B., Foley, J.A., Pollard, D., Levis, S., 2004. Decadal variability of rainfall in the Sahel: results from the coupled GENESIS-IBIS atmosphere–biosphere model. *Clim. Dyn.* 22, 625–637.
- Warner, R.C., Budd, W.F., 1998. Modelling the long-term response of the Antarctic ice sheet to global warming. *Ann. Glaciol.* 27, 161–168.
- Wilch, E., Hughes, T.J., 2000. Calculating basal thermal zones beneath the Antarctic ice sheet. *J. Glaciol.* 46, 297–310.
- Zachos, J.C., Quinn, T.M., Salmay, K.A., 1996. High-resolution (10⁴ years) deep-sea foraminiferal stable isotope records of the Eocene–Oligocene climate transition. *Paleoceanography* 11, 251–266.
- Zachos, J., Pagani, M., Sloan, L., Thomas, E., Billups, K., 2001. Trends, rhythms, and aberrations in global climate 65 Ma to present. *Science* 292, 686–693.